Journal of Inclusion Phenomena and Molecular Recognition in Chemistry **25:** 327–338, 1996.

Interactions Between Naproxen and Maltoheptaose, the Non-Cyclic Analog of β-Cyclodextrin

G. P. BETTINETTI[1],* P. MURA[2], F. MELANI[2], M. RILLOSI[1] and F. GIORDANO[3]

[1]*Dipartimento di Chimica Farmaceutica, Università di Pavia, Viale Taramelli 12, I-27100 PV, Italy.*
[2]*Dipartimento di Scienze Farrnaceutiche, Università di Firenze, Via G. Capponi 9, I-50121 FI, Italy.*
[3]*Dipartimento Farmaceutico, Università di Parma, Viale delle Scienze, I-43100 PR, Italy.*

(Received: 15 December 1995; in final form: 19 April 1996)

Abstract. The crystallinity of naproxen in solid combinations with amorphous maltoheptaose, the non-cyclic analog of β-cyclodextrin, was assessed using differential scanning calorimetry supported by X-ray powder diffractometry. Cogrinding induced a decrease in drug crystallinity to an extent which depended on the grinding time, and was most pronounced for the combination of equimolecular composition. Thermal analysis showed that the mechanism behind the conversion of crystalline naproxen into the amorphous state by cogrinding with maltoheptaose differed from that with randomly substituted, amorphous β-cyclodextrins. Interactions of naproxen with maltoheptaose in aqueous solution were studied by means of fluorescence spectroscopy, phase-solubility analysis, and computer-aided molecular modelling. Maltoheptaose can wrap up naproxen, taking on a cyclic conformation and forming a 'pseudo' inclusion complex (apparent binding constant $K_{1:1} = 1.0 \times 10^3$ (±20%) L mol^{-1} at 25 °C) which is about as stable as the true inclusion complex with β-cyclodextrin in the lowest temperature range (0–100 K). A better complexing ability for naproxen in terms of binding constant values, however, was displayed by both native and derivatized β-cyclodextrins, the 'hosts' with covalently-bound cyclic structures.

Key words: Maltoheptaose, naproxen, naproxen-maltoheptaose blends, grinding, crystallinity, complexation, thermal analysis, X-ray diffractometry, molecular modelling.

1. Introduction

The shift from the poorly water-soluble ($<0.02 g/g_{water}$ at room temperature) natural β-cyclodextrin to the more soluble ($>0.5 g/g_{water}$) chemically-modified β-cyclodextrins improves the pharmaceutical usefulness of these host substances as solubilising, dissolution rate-enhancing, and complexing agents for the naproxen guest molecule, a potent non-steroidal antiinflammatory drug with very poor water solubility [1–4]. Moreover, random substitution of β-cyclodextrin results in the amorphous state, which in turn may be conferred on crystalline naproxen in solid combinations [1–4]. Since maltoheptaose, the noncyclic analog of β-cyclodextrin, or 'open' β-cyclodextrin, is also amorphous, a study of the naproxen-maltoheptaose system in the solid state and in aqueous solution was undertaken, using differential scanning calorimetry supported by X-ray powder diffractometry, and fluorescence

* Author for correspondence.

spectroscopy, phase-solubility diagrams, and computer-assisted molecular graphics. The results in terms of naproxen–maltoheptaose interactions in the solid (drug amorphisation) and liquid (drug solubilisation) states are discussed and compared with those previously obtained with some amorphous β-cyclodextrins and with crystalline native β-cyclodextrin, in order to obtain direct information on the relevance of the cyclic structure in these interactions.

2. Experimental

2.1. MATERIALS

Naproxen (NAP) ((*S*)-(+)-6-methoxy-α-methyl-2-naphthaleneacetic acid) from Sigma Chemical Co, St. Louis, MO (USA) and maltoheptaose (MHEPT) from Nihon Shokuhin Kako Co. Ltd. (Japan) were used. The structure of NAP and MHEPT molecules is shown in Scheme 1.

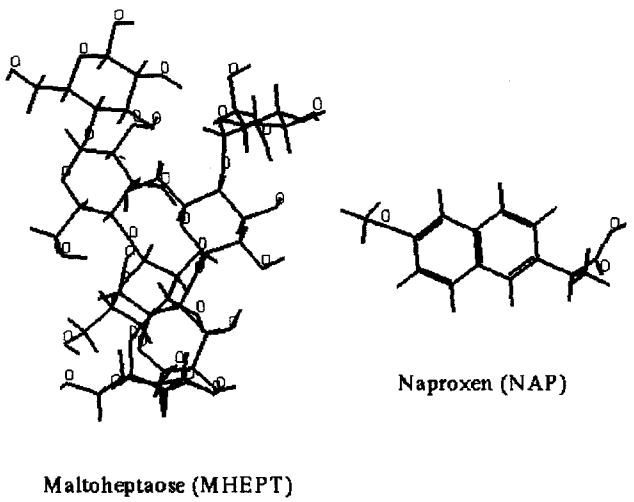

Scheme 1.

Blends of NAP (75–150 μm sieve granulometric fraction) and MHEPT at the 0.27, 0.15, 0.084, and 0.058 mass fractions of NAP were formed by turbula mixing for 10 min. The total weight of each specimen varied from 50 to 350 mg. The blends were manually ground using an agate mortar with a pestle, then tested by differential scanning calorimetry (DSC) and X-ray powder diffractometry (see below) after grinding times of 0, 10, 20, 30, and 40 min. The same mechanical treatment was performed on crystals of pure NAP for control purposes. Thin layer chromatographic (TLC) analysis [5] indicated that NAP was not subject to chemical decomposition under the grinding conditions.

2.2. THERMAL ANALYSIS

Temperature and enthalpy measurements were carried out with a Mettler TA4000 apparatus equipped with a differential scanning calorimetric (DSC) 25 cell (10 K min^{-1}, 30–180 °C) on 3.5–5.0 mg (Mettler M3 microbalance) samples in open alumina pans under static air. Thermogravimetric analysis (TGA) was conducted on a Mettler TG 50 apparatus (10 K min^{-1}, 30–300 °C) on 5–7 mg samples in open alumina crucibles under a nitrogen atmosphere (10 mL min^{-1}).

2.3. POWDER X-RAY DIFFRACTOMETRY

X-ray powder diffraction patterns were recorded with a computer-controlled Philips PW 1800 apparatus over the 2–40° 2θ range at a scan rate of 1° min^{-1}, using CuK_α radiation monochromatized with a graphite crystal.

2.4. SOLUBILITY STUDIES

Solubility measurements of NAP were performed in duplicate by adding 30 mg of drug to 30 mL of water or aqueous solution of MHEPT in the 1.0 to 10.0 mmol L^{-1} concentration range, in a sealed glass container which was electromagnetically stirred at a constant temperature (25 ± 0.5 °C) until equilibrium was achieved. An aliquot was withdrawn, and the NAP concentration was determined as described previously [6, 7]. The apparent binding constant of the NAP–MHEPT complex was calculated from the slope and intercept of the straight line of the phase-solubility diagram, in terms of Equation (1) [8].

$$K_{1:1} = \frac{\text{slope}}{\text{intercept}(1 - \text{slope})} \tag{1}$$

2.5. FLUORESCENCE SPECTRA

Measurements were carried out using a Perkin Elmer Model 650-10 S spectrofluorimeter. The fluorescence intensities of the 1.2 μM NAP aqueous solution as such and in the presence of either MHEPT or β-cyclodextrin (βCD) at concentrations of 80 and 280 μmol L^{-1} were measured at excitation and emission maxima of 330 and 358 nm, respectively.

2.6. MOLECULAR MODELLING

MHEPT is a linear oligomer composed of seven glucose units linked by α-1,4 linkages, which can be considered the noncyclic analog of native βCD, i.e. the 'open' βCD. The structure of MHEPT was determined through its binding to phosphorylase and was found to be a left-handed helix, with 6.5 glucose residues per turn and a rise per residue of 2.4 Å [9]. Short-chain amyloses of precise chain lengths

are potential supermolecules, since a guest molecule can enter the intrahelical channel and form a 'pseudo' inclusion complex [10]. The molecules of NAP and MHEPT were created, as described previously [2–4], using the proper Builder Module of the INSIGHT 2.2.0 program (Byosim Technologies [11]). Analysis and modelling of the structure of the NAP–MHEPT 'inclusion' complex were carried out using the same INSIGHT 2.2.0 program [11]. Each structure was subjected to a process of energy minimization (AMBER force field, DISCOVER 2.9 program [11]), performing iterations to a <0.05 derivative value. Molecular dynamic simulations were carried out at five temperatures under the following experimental conditions: time step 1 fs, equilibrium time 1000 fs, step number 100 000). Docking energies were calculated at 0 K (rigid molecule) and at 100, 200, 300 and 400 K, averaging the energies of 90 conformations generated during the dynamic molecular program (5 to 10 ps) in the last four cases. The role of the water molecules in the NAP–MHEPT interaction could not be taken into account in docking calculations, due to the excessive amount of computer time required at present by such an approach.

3. Results and Discussion

3.1. INTERACTION IN THE SOLID STATE

The thermal behaviour of the single components is shown in Figure 1. A sharp endothermal effect (t_{onset} = 153.4 °C, t_{peak} = 156.7 °C, fusion enthalpy 140 J g^{-1} [12]) was associated with the melting of anhydrous crystals of pure NAP (Figure 1a), while only a large endothermal effect (temperature range 35–125 °C, t_{peak} = 49.3 °C, $\Delta H \approx 150$ J g^{-1}) due to dehydration was recorded for amorphous, hygroscopic MHEPT (Figure 1b). TGA and derivative thermogravimetric (DTG) curves indicated a mass loss of MHEPT in the same temperature range of the DSC dehydration endotherm due to water evolution (Figure 1b). The first step (8% as mass fraction) corresponded to the water evolution (0.080 mass fraction of water), followed by a mass loss which started from 200 °C and was attributable to sample decomposition (Figures 1c and 1d).

The results of DSC analysis of NAP and its combinations with MHEPT at 0.27, 0.15, 0.084, and 0.058 mass fraction of NAP are presented in Figure 2 and Table I. The melting peak of NAP (see Figure 1a) was substantially unaffected in its shape and area by blending with MHEPT (Figure 2) or by grinding the crystals of pure NAP (Table I). Except for the combination containing the 0.27 mass fraction of NAP (i.e. 2 NAP moles per MHEPT mole), a decrease in the fusion enthalpy per unit mass of NAP (i.e. in drug crystallinity) was evident in ground mixtures. The loss of drug crystallinity due to the cogrinding effect was directly related to the duration of mechanical treatment and led to asymmetry of the melting peak of NAP (indicated by the lower onset temperatures in Table I) after grinding times of 20 min or longer. In all the combinations with MHEPT the peak temperature was substantially that of pure NAP, despite peak asymmetry. Instead, in systems of NAP with amorphous hydroxypropyl and hydroxyethyl derivatives of βCD, decreases

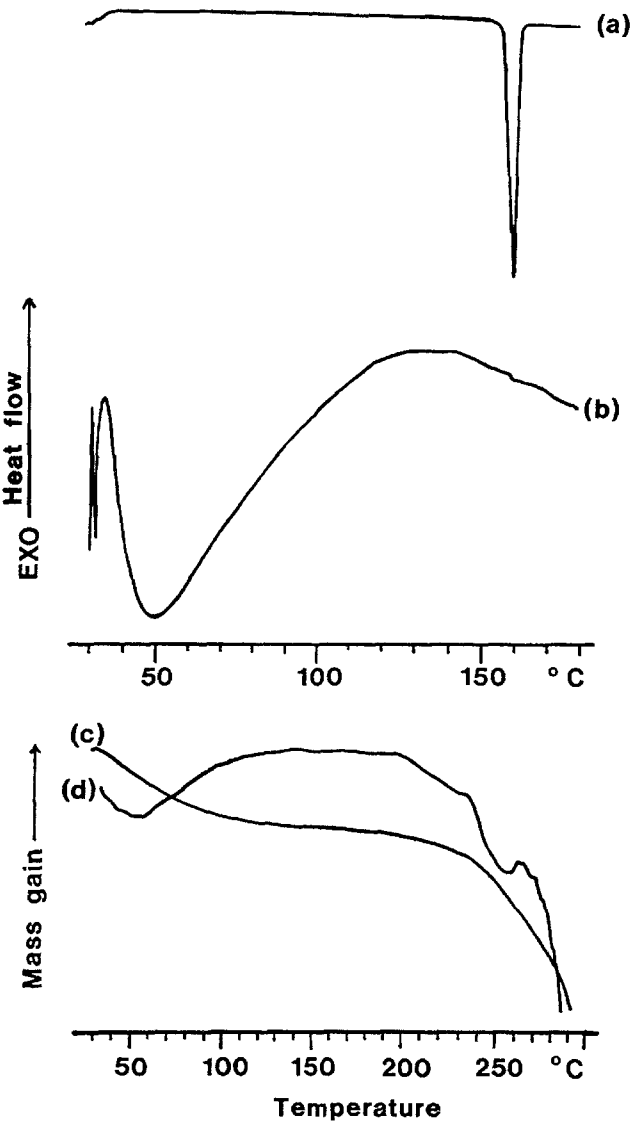

Figure 1. DSC curves of naproxen (NAP) (a) and maltoheptaose (MHEPT) (b), and TGA (c) and DTG (d) curves of MHEPT.

in the melting peak area of the drug were always associated with drops in peak temperature (to 135 °C) [3, 4]. The mechanism behind the NAP amorphisation by cogrinding with a random-substituted βCD therefore seemed different from that with MHEPT, and probably involved the inclusion of NAP into the macrocyclic cavity in the solid state.

As far as the extent of NAP amorphisation as a function of grinding time in the various combinations with MHEPT is concerned, complete amorphisation was

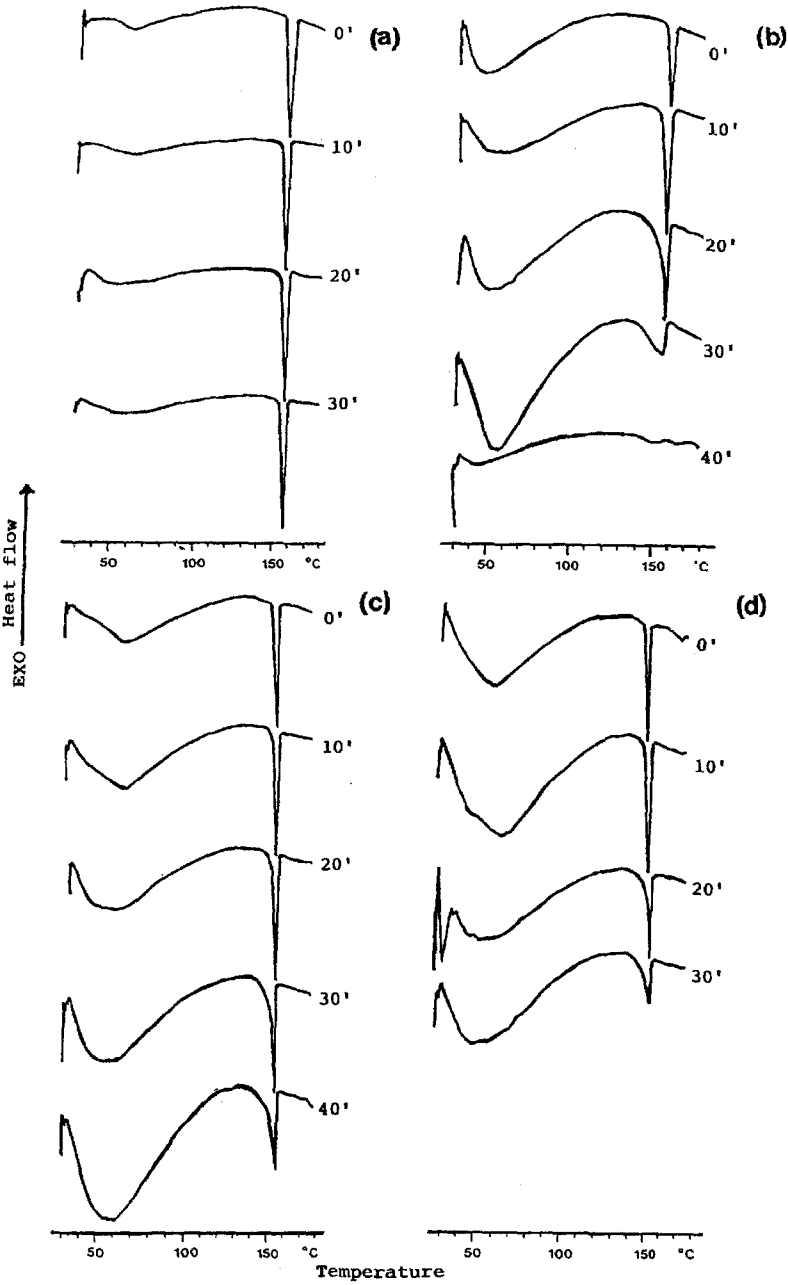

Figure 2. DSC curves of blended and ground mixtures of naproxen (NAP) and maltoheptaose (MHEPT) at 0.27 (a), 0.15 (b), 0.084 (c), and 0.058 (d) mass fraction of NAP (grinding time (min) on the curves).

Table I. Effect of grinding on the DSC fusion endotherm of naproxen (NAP) alone or in combinations with maltoheptaose (MHEPT).

Sample	Mass fraction of NAP	Grinding time (min)	Onset temperature (°C)	Peak temperature (°C)	NAP crystallinity (% of NAP mass fraction)
NAP	1	0	153.4	156.7	100
NAP	1	10	153.5	156.7	99
NAP	1	20	152.5	156.5	99
NAP	1	30	152.7	156.2	100
NAP/MHEPT	0.27	0	153.0	156.7	100
NAP/MHEPT	0.27	10	151.0	156.3	100
NAP/MHEPT	0.27	20	151.0	156.3	99
NAP/MHEPT	0.27	30	150.1	156.4	96
NAP/MHEPT	0.15	0	152.1	156.7	100
NAP/MHEPT	0.15	10	150.4	155.9	92
NAP/MHEPT	0.15	20	141.4	155.3	70
NAP/MHEPT	0.15	30	134.3	154.0	38
NAP/MHEPT	0.15	40	–	–	0
NAP/MHEPT	0.084	0	153.2	156.5	100
NAP/MHEPT	0.084	10	149.9	156.6	94
NAP/MHEPT	0.084	20	147.6	155.9	91
NAP/MHEPT	0.084	30	146.1	156.0	80
NAP/MHEPT	0.084	40	140.7	155.3	58
NAP/MHEPT	0.058	0	150.5	156.6	100
NAP/MHEPT	0.058	10	149.6	156.0	96
NAP/MHEPT	0.058	20	147.5	155.8	90
NAP/MHEPT	0.058	30	138.6	156.0	77

achieved after 40 min grinding only for the mixture containing the 0.15 mass fraction of NAP, which corresponded to the equimolecular ratio of drug and carrier (Table I).

X-ray powder diffraction patterns of NAP, MHEPT, and some of their combinations at the 0.27 and 0.15 mass fractions of NAP are displayed in Figure 3. In the NAP–MHEPT blends, the strongest diffraction peaks of pure NAP, corresponding to the theoretical ones calculated from single crystal data (reference pattern No. 40-1555 (1994) of JCPDS (Joint Committee on Powder Diffraction Standards)), emerged on the diffuse background of amorphous MHEPT. Cogrinding of the mixtures containing the 0.15 mass fraction of NAP induced a sharp decrease in peak intensity, and after 40 min led to amorphisation of all the NAP present (Figure 3f), in agreement with the DSC results.

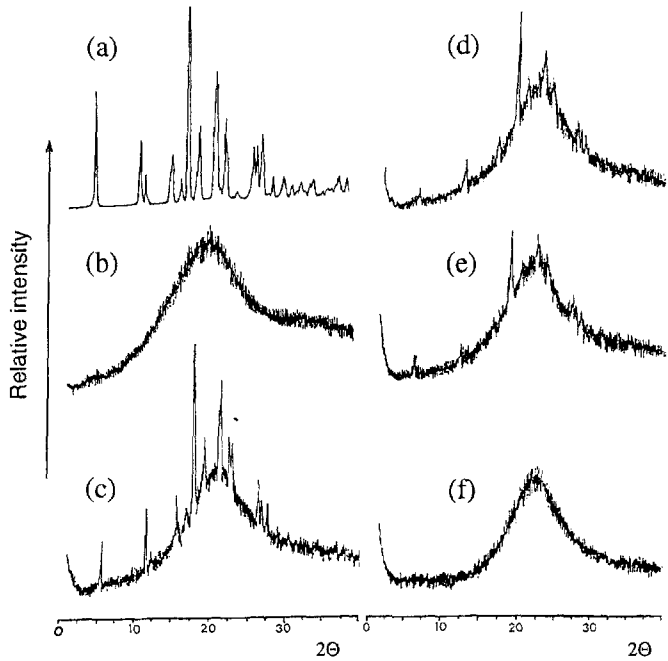

Figure 3. Powder X-ray diffraction patterns of naproxen (NAP) (a), maltoheptaose (MHEPT) (b), NAP–MHEPT blend at 0.27 mass fraction of NAP (c) and NAP–MHEPT mixture at 0.15 mass fraction of NAP ground for 10 (d), 20 (e), and 40 (f) min.

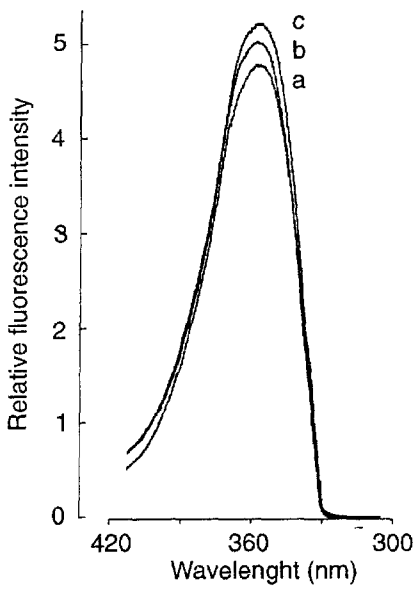

Figure 4. Effect of maltoheptaose (MHEPT) and β-cyclodextrin (βCD) on the fluorescence spectrum of naproxen (c(NAP) = 1.2 μmol L^{-1}). NAP in water (curve a), in 80 μM aqueous solution of MHEPT (curve b), and in 80 μM aqueous solution of βCD (curve c).

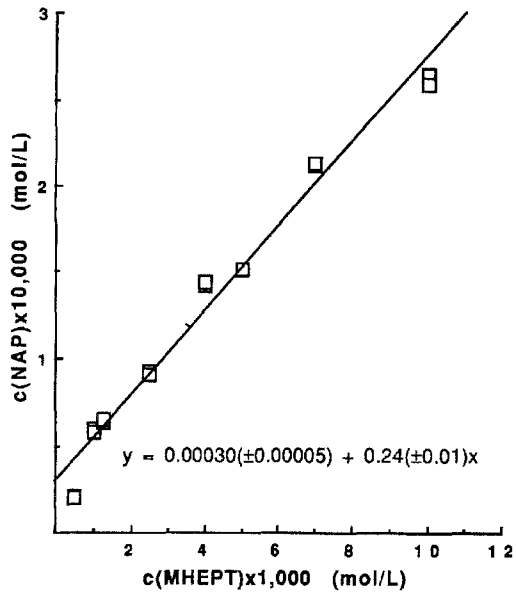

Figure 5. Phase-solubility diagram of naproxen (NAP) and maltoheptaose (MHEPT) in water at 25 °C.

3.2. INTERACTION IN AQUEOUS SOLUTION

The formation of a 'pseudo' inclusion compound between MHEPT and NAP in aqueous solution was demonstrated by fluorescence and phase-solubility analyses. The enhancement of fluorescence of NAP in the presence of MHEPT, however, was lower than that observed with βCD at the same concentration level as MHETP (Figure 4). This suggests a better fit of the NAP molecule within the CD macrocycle than inside the MHETP helicoidal structure. In the MHETP system a more gently sloping A_L-type diagram than in the βCD systems [2–4, 6, 7] was obtained (Figure 5), indicating a weaker interaction between the drug and the carrier. The apparent binding constant ($K_{1:1} = 1.0 \times 10^3 \pm 20\%$ L mol^{-1} at 25 °C) actually shows a lower complex-forming ability toward NAP of the noncyclic analog MHEPT than the corresponding covalently-bound, cyclic structure of native βCD ($K_{1:1} = 1.7 \times 10^3 \pm 17\%$ L mol^{-1} at 25 °C [6]) and its derivatives ($K_{1:1} = 2.2 \times 10^3 \pm 14\%$ to $6.2 \times 10^3 \pm 11\%$ L mol^{-1} at 25 °C [2–4, 7]). Analogous differences in 'strength' of complexation between native βCD and MHEPT towards 4-nitrophenolate ion and methyl orange have been reported [13]. These differences can mostly be ascribed to an absence in NAP–βCD interactions of energy requirements for the formation of cyclic conformations, which are essential for the NAP–MHETP interaction.

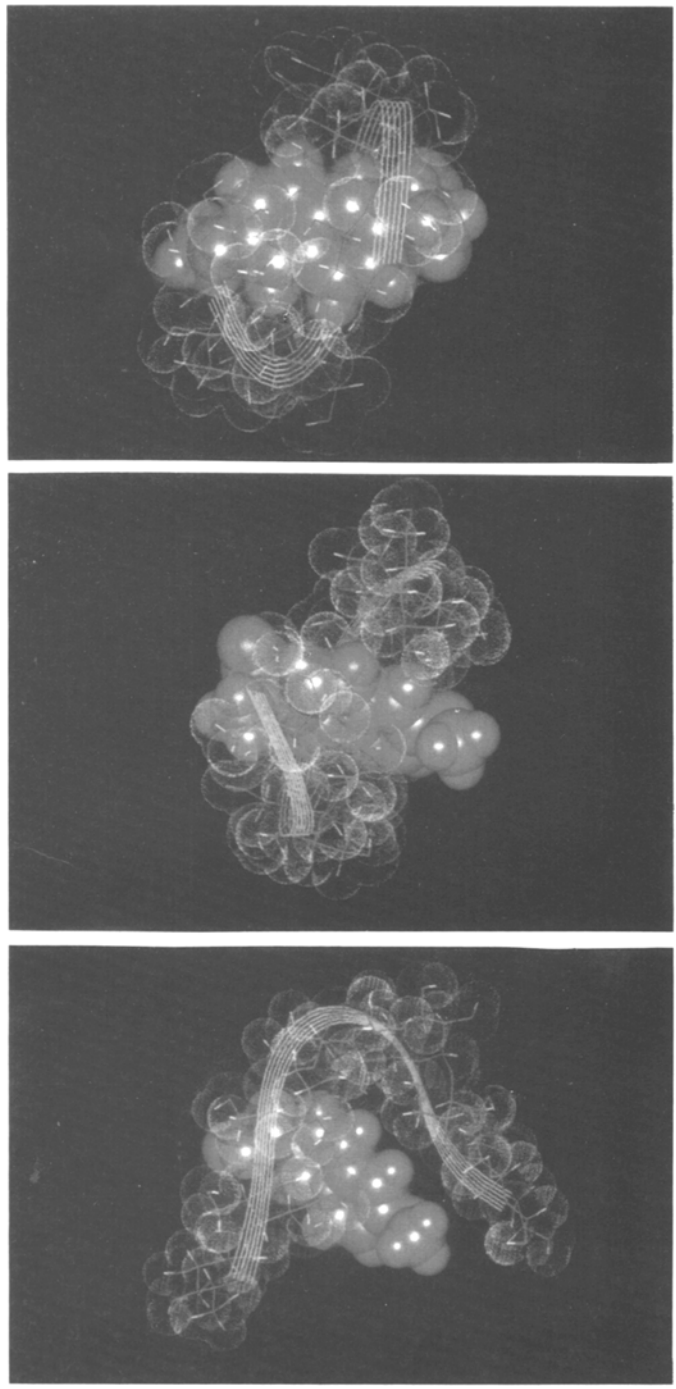

Figure 6. Computer-generated 'pseudo' inclusion complex between naproxen (NAP) and maltoheptaose (MHEPT) at (a) 0, (b) 200, and (c) 400 K.

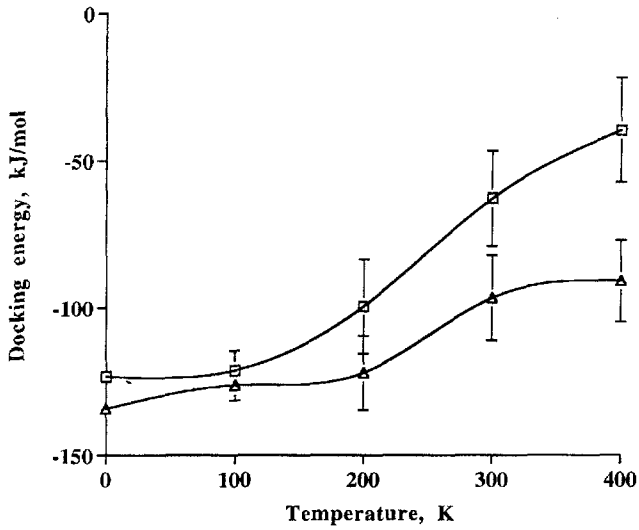

Figure 7. Influence of temperature on the docking energy values for the naproxen (NAP)–maltoheptaose (MHEPT) (□) and NAP–β-cyclodextrin (βCD) (△) interactions (bars indicate standard deviation).

3.3. MOLECULAR MODELLING

Molecular modelling showed that the linear analogue of βCD may have the feature of a supermolecule for NAP, accounting for the rather stable complex formed in aqueous solution, since MHETP can wrap up NAP, adopting a quasi-cyclic conformation with no large strains in the bonds between the glucoside residues (Figure 6). Docking energy values calculated at 0, 100, 200, 300 and 400 K show that the NAP–MHETP 'pseudo' inclusion complex was rather less stable than the true one with βCD (Figure 7). The differences between the docking energies of the NAP–MHETP and NAP–βCD interactions were statistically significant at the $P < 0.01$ level at temperatures of 200, 300, 400 K and at the $P < 0.5$ level at the temperature of 100 K. Moving towards the higher temperatures, a marked decrease in the stability of the 'pseudo' inclusion complex was evident. This might be attributed to an increase in molecular mobility, with consequent opening of the helicoidal conformation of MHETP and loosening of the NAP wrapping-up by MHETP (see Figure 6c).

4. Conclusion

Despite the amorphising and solubilising properties exhibited by MHEPT, its pharmaceutical application as a drug carrier can not to be proposed at present, due to its prohibitive price (about 250 times more expensive than βCD). A comparative study of the interactions of drugs with MHEPT or maltohexaose (the 'open' α-cyclodextrin) and the respective cyclic derivatives can be however of theoret-

ical interest from the point of view of the supramolecular chemistry. In a recent paper, for example, the results of ionspray and tandem-mass spectroscopy experiments on mixtures of piroxicam with βCD or maltohexaose supported that the 1 : 1 drug/βCD adducts previously detected were true inclusion complexes rather than ion-molecule clusters [14].

Acknowledgements

Financial support from the MURST (funds 60%) and CNR to GPB is gratefully acknowledged. The authors wish to thank Mrs. M.C. Sacchi for her skilful technical assistance.

References

1. G.P. Bettinetti, A. Gazzaniga, P. Mura, F. Giordano and M. Setti: *Drug Dev. Ind. Pharm.* **18**, 39 (1992).
2. G.P. Bettinetti, P. Mura, F. Melani and F. Giordano: *Proc. 7th Intern. Cyclodextrins Symp.* (Acad. Soc. Japan, Tokyo), p. 455 (1994).
3. P. Mura, G.P. Bettinetti, F. Melani and A. Manderioli: *Eur. J. Pharm. Sci.* **3**, 347 (1995).
4. F. Melani, G.P. Bettinetti, P. Mura and A. Manderioli: *J. Incl. Phenom.* **22**, 131 (1995).
5. F.J. Al-Shammary, N.A.A. Mian and M.S. Mian: in H.G. Brittain (ed.), *Analytical Profiles of Drug Substances and Excipients*, Vol. 21, Academic Press pp. 345–373, (1992).
6. G.P. Bettinetti, P. Mura, A. Liguori, G. Bramanti and F. Giordano: *Il Farmaco* **44**, 195 (1989).
7. G.P. Bettinetti, F. Melani, P. Mura, R. Monnanni and F. Giordano: *J. Pharm. Sci.* **80**, 1162 (1991).
8. T. Higuchi and K.A. Connors: *Adv. Anal. Chem. Instr.* **4**, 117 (1965)
9. E. Goldsmith, S. Sprang and R. Fletterick: *J. Mol. Biol.* **156**, 411 (1982).
10. D. Vetter: Workshop on Supramolecular Organic Chemistry and Photochemistry, Saarbrucken (FRG), *Book of Abstracts*, P64 (1989).
11. Byosim Technologies, 9685 Scranton Road, S. Diego, CA 92121-2777.
12. G.P. Bettinetti, P. Mura, F. Giordano and M. Setti: *Thermochim. Acta* **199**, 165 (1991).
13. M. Komiyama and H. Hirai: *Makromol. Chem. Rapid Commun.* **7**, 739 (1986).
14. A. Selva, E. Redenti, M. Zanol, P. Ventura and B. Casetta: *Eur. Mass Spectrom.* **1**, 105 (1995).